Available online at website: https://journal.bcrec.id/index.php/bcrec

Bulletin of Chemical Reaction Engineering & Catalysis, 21 (3) 2026, 683-696

Original Research Article

Catalytic Aromatization of Propane-Butane Fractions over Polyfunctional Zeolite Catalysts: Effect of Process Parameters

Nurzhan Nurgaliyev[1], Nur-Sultan Mussa[2], Seitkhan Azat[3], Rachid Amrousse[4], Kainaubek Toshtay[2,*]

[1]Shakarim University, Glinki, 20, Semey, Kazakhstan.
[2]Al-Farabi Kazakh National University, Al-Farabi 71, 050040, Almaty, Kazakhstan.
[3]Satbayev University, Satbayev Str. 22, Almaty, 050000, Kazakhstan.
[4]Chouaïb Doukkali University, Faculty of Sciences, 24000 El Jadida, Morocco.

Received: 10th February 2026; Revised: 29th May 2026; Accepted: 29th May 2026
Available online: 20th June 2026; Published regularly: October 2026

Abstract

The catalytic conversion of a propane–butane fraction into aromatic hydrocarbons was investigated over ZnLaFe/ZSM-5 and phosphorus-modified ZnLaFeP/ZSM-5 catalysts. The catalysts were characterized by N_2 adsorption–desorption, X-ray diffraction, SEM-EDX, TEM, NH_3-TPD, TGA and FTIR-pyridine analyses. Textural and structural studies confirmed the preservation of the MFI framework after metal and phosphorus incorporation, while acidity measurements revealed that phosphorus modification significantly reduced the concentration of medium-strong and strong Brønsted acid sites, leading to a moderated acid strength distribution. Catalytic performance tests demonstrated that ZnLaFe/ZSM-5 exhibits high PBF conversion over a wide temperature range, whereas ZnLaFeP/ZSM-5 delivers substantially higher aromatic yields, reaching up to 59.7% at 550 °C and a gas hourly space velocity (GHSV) of 350 h^{-1}. The enhanced aromatization performance of the phosphorus-containing catalyst is attributed to the synergistic interaction between moderated Brønsted acidity and Zn–phosphate Lewis acid sites, which promote dehydrogenation, cyclization, and aromatization while suppressing excessive cracking and coke formation. Stability tests over 11 h confirmed the superior resistance of ZnLaFeP/ZSM-5 to deactivation, with only minor losses in conversion and aromatic yield and a stable product distribution dominated by benzene and toluene. Pilot-scale experiments using larger catalyst beds (100 and 500 mL) further demonstrated that the optimized acidity and catalytic functionality are retained upon scale-up.

Copyright © 2026 by Authors, Published by BCREC Publishing Group. This is an open access article under the CC BY-SA License (https://creativecommons.org/licenses/by-sa/4.0).

Keywords: propane-butane fraction ; liquefied petroleum gas ; catalyst ; ZSM-5 ; aromatic compound

How to Cite: Nurgaliyev, N., Mussa, N., Azat, S., Amrousse, R., Toshtay, K. (2026). Catalytic Aromatization of Propane-Butane Fractions over Polyfunctional Zeolite Catalysts: Effect of Process Parameters. *Bulletin of Chemical Reaction Engineering & Catalysis*, 21 (3), 683-696. (DOI: 10.9767/bcrec.20667)

Permalink/DOI: https://doi.org/10.9767/bcrec.20667

1. Introduction

Aromatic hydrocarbons are key building blocks for the production of synthetic polymers, pharmaceuticals, agrochemicals, and a wide range of other high-value chemical products. By the end of 2025, global demand for aromatics had increased by nearly 40%, reaching approximately 169 million tons. This rapid growth highlights the strategic importance of developing more efficient and sustainable routes for aromatic hydrocarbon production [1]. Traditionally, aromatics are obtained mainly through catalytic reforming and high-temperature cracking of naphtha. However, rising demand, together with increasing environmental and economic pressures, has encouraged the exploration of alternative feedstocks and conversion technologies.

Liquefied petroleum gas (LPG), particularly propane–butane fractions, has gained attention as a promising feedstock for the production of valuable aromatic hydrocarbons such as benzene, toluene, and xylenes [2,3]. Despite its availability,

* Corresponding Authors.
Email: kainaubek.toshtay@kaznu.kz (K. Toshtay)

significant amounts of LPG are still flared during oil and gas production and processing, leading to substantial carbon losses and unnecessary greenhouse gas emissions. In this regard, catalytic aromatization of LPG represents an attractive strategy to improve carbon utilization, reduce emissions, and simultaneously generate high-value aromatic products [4,5].

Current industrial catalysts for propane dehydrogenation are primarily based on Pt or CrO_x supported on Al_2O_3 [6–8]. Although these systems are widely used, they suffer from rapid deactivation, declining olefin selectivity during extended operation, and, in the case of Pt-based catalysts, high material costs [9–13]. These limitations clearly indicate the need for more efficient, selective, and durable catalytic systems for industrial aromatization processes [14]. ZSM-5 zeolite has been extensively investigated as a catalyst support for light-alkane aromatization due to its adjustable acidity, well-defined pore structure, and high thermal stability. Nevertheless, the strong Brønsted acidity of unmodified ZSM-5 often promotes excessive cracking and coke formation, which negatively affects aromatic selectivity and catalyst lifetime [15,16]. To address these issues, ZSM-5 has been modified with various metal species, including Ga, Zn, Pt, Mo, Mg, Cu, and Fe, which are known to enhance dehydrogenation activity and suppress undesired side reactions. In many cases, polymetallic modification has been shown to provide higher catalytic activity and improved thermal stability compared to monometallic systems [17].

Several studies have demonstrated the beneficial role of Zn in aromatization catalysts [18–20]. Increasing Zn loading has been reported to enhance aromatic selectivity by increasing the number of dehydrogenation-active sites that favor cyclization and aromatization pathways [21]. Structural modification of ZSM-5 through desilication has also been shown to significantly improve benzene, toluene, and xylene (BTX) selectivity, which has been attributed to increased acidity and the formation of additional mesoporosity that facilitates molecular diffusion. Furthermore, catalysts in which Zn species are located within the zeolite micropores while metallic Ni particles are preferentially located on the external surface exhibit enhanced aromatic selectivity [22]. This spatial separation reduces excessive hydrogenation activity and allows intermediate olefins to undergo cyclization and subsequent aromatization [23–25].

The incorporation of additional promoters has also proven effective. Rare-earth elements such as La have been shown to increase the concentration of catalytically active Zn species, leading to improved aromatic selectivity [26]. Co-modification with phosphorus further enhances aromatic yields by moderating acid strength and improving catalyst stability [27]. Similarly, the addition of Fe to Mo-based ZSM-5 catalysts has been reported to increase benzene formation and slow catalyst deactivation, which has been attributed to the formation of carbon nanostructures that improve mass transport and delay pore blockage[28]. Despite these advances, ZSM-5-based catalysts remain constrained by their intrinsic microporous structure, which can limit metal dispersion and restrict the diffusion of bulky aromatic molecules. These limitations often lead to rapid catalyst deactivation during prolonged operation. Among various modification strategies, phosphorus incorporation is widely recognized as an effective approach to improve catalyst stability by moderating acidity and enhancing resistance to coke formation under severe reaction conditions [29–31].

Accordingly, in the present study, phosphorus was introduced into ZnLaFe/ZSM-5 catalysts and their performance in propane–butane aromatization was investigated. The combined modification with Zn, La, Fe, and P was found to enhance dehydrogenation activity, regulate zeolite acidity, and improve metal–support interactions, leading to more effective bifunctional catalysis. Phosphorus and lanthanum played a key role in stabilizing the zeolite framework, limiting metal migration, and suppressing coke formation, which resulted in improved catalytic stability and prolonged lifetime. Overall, the co-modified ZSM-5 catalysts exhibited enhanced activity and aromatic selectivity, demonstrating that controlled multi-element modification is an effective strategy for developing stable and efficient catalysts for light alkane aromatization.

2. Materials and Method

2.1. Materials

ZSM-5 zeolite (HJI Co. LTD, China) was used as the catalyst support. Zinc nitrate monohydrate ($Zn(NO_3)_2 \cdot H_2O$, Sigma-Aldrich), lanthanum(III) nitrate hexahydrate ($La(NO_3)_3 \cdot 6H_2O$, Sigma-Aldrich), iron(III) nitrate nonahydrate ($Fe(NO_3)_3 \cdot 9H_2O$, Sigma-Aldrich), and ortho-phosphoric acid (85% H_3PO_4, Sigma-Aldrich) were used as the precursors for Zn, La, and P, respectively.

2.2. Catalyst Synthesis

The ZnLaFe/ZSM-5 and ZnLaFeP/ZSM-5 catalysts were prepared by the incipient wetness impregnation method using ZSM-5 as the support. Appropriate amounts of zinc, lanthanum, iron, and phosphorus precursors were dissolved in deionized water to form an aqueous solution with pH = 5. The total solution volume was matched to the pore volume of the ZSM-5 support to ensure complete impregnation. The precursor solution

Copyright © 2026, ISSN 1978-2993

was added dropwise to the support under continuous stirring to achieve uniform distribution of the active components. The impregnated samples were aged at room temperature for 12 h, followed by drying in static air at 150 °C for 12 h. The dried materials were then calcined in ambient air at 550 °C for 5 h (heating rate: 5 °C.min^{-1}). The final catalysts contained 3 wt% Zn, 1.5 wt% La, 0.5 wt% Fe, and 1 wt% P (for the P-modified sample), and were designated as ZnLaFe/ZSM-5 and ZnLaFeP/ZSM-5, respectively.

2.3. Characterizations of Samples

The textural characteristics of the studied samples were determined using the nitrogen adsorption-desorption method on a BeiShiDe Instrument Co., Ltd, 3H-2000PM2 device (China) at a temperature of -196 °C. The measurements were performed after preliminary degassing of the samples at 380 °C for 5 hours. The specific surface area of the samples was determined using the Brunauer-Emmett-Teller (BET) method. The pore size distribution was determined using the Barrett-Joyner-Halenda (BJH) method. The acidity of the catalysts was investigated using the temperature-programmed desorption of ammonia (TPD-NH_3) method on an AutoChem 2950HP device (Micromeritics). X-ray diffraction data were acquired using a Shimadzu XRD-7000 diffractometer operated in reflection mode and equipped with a Cu-Kα radiation source. Diffraction scans were recorded across a 2θ interval of 5–50° using a scan speed of 5° min^{-1}. The surface morphology of the obtained catalysts was examined by scanning electron microscopy (SEM) using a Hitachi S-3400N II instrument. The structure of the catalysts was investigated using a transmission electron microscope (TEM) JEM-2100 (JEOL, Japan) with an image resolution of 0.19 nm at an accelerating voltage of 200 kV. Infrared spectra of adsorbed pyridine were recorded using a Bruker Tensor 27 FT-IR spectrometer (Karlsruhe, Germany) to identify the acid types of the catalysts. Thermogravimetric analysis (TGA) analysis of the coked catalysts was performed using a Perkin Elmer TGA-4000 instrument under an air atmosphere to determine coke content after the aromatization reaction. About 10 mg of sample was heated in flowing air (20 mL/min) from 35 to 900 °C at a heating rate of 10 °C/min.

2.4. Experimental Setup and Product Analysis

Conversion of the propane-butane fraction (ratio propane-butane) was carried out in a continuous-flow fixed-bed quartz reactor operated at atmospheric pressure. Catalyst (5 g) was placed between two layers of quartz. Reaction temperatures ranged from 450 to 600 °C, and the gas hourly space velocity (GHSV) was set between 140 and 500 h^{-1}. The schematic diagram of the flow reactor is shown in Figure 1.

After catalyst loading, activation was conducted by passing air through the reactor for 1 h. Argon was then introduced for 15 min to remove residual air, and propane-butane fraction was subsequently supplied. Catalyst bed temperature was monitored using a chromel-alumel thermocouple, and operating conditions were

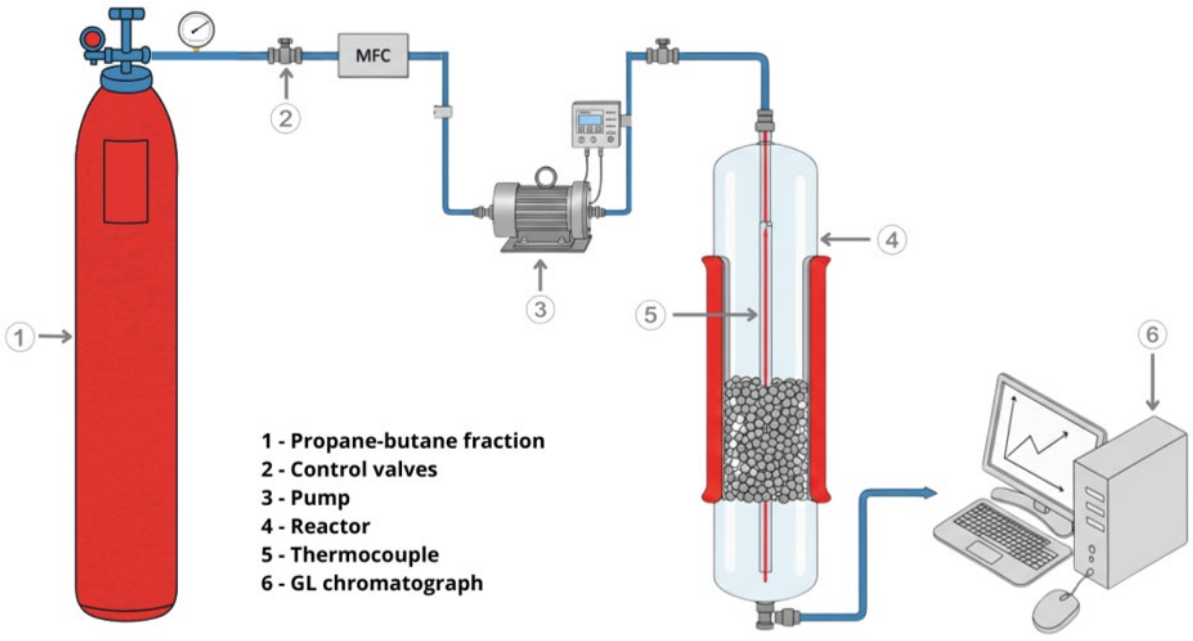

Figure 1. Schematic diagram of a flow setup for converting propane-butane fraction into aromatic compounds.

Copyright © 2026, ISSN 1978-2993

controlled with a voltage regulator. Feedstock delivery was maintained at the specified rate, with distilled water flow regulated by a pump. The gaseous products were cooled in a condenser and collected as liquid in the product receiver. The composition of the reaction gas products was analyzed by gas-liquid chromatography (GL) using a Chrom-5 chromatograph (Hungary) equipped with an alumina-packed column (3 m length, 4 mm diameter, 50-250 °C range). Liquid organic products (aromatic compounds) were further analyzed on an Agilent 6890 system (USA) with FID, using a 60 m × 0.25 mm capillary column (PDMS coating, 50-350 °C range) and helium as the carrier gas.

The conversion of propane-butane fraction (X, %) is calculated using the following formula:

$$X = \frac{C_{in} - C_{out}}{C_{in}} \times 100\% \quad (1)$$

where, C_{in} and C_{out} are the concentrations of the reactants at inlet and outlet respectively. The yield of aromatic hydrocarbons (Y, %) is then determined according to:

$$Y = \frac{C_{ArC}}{C_{in}} \times 100\% \quad (2)$$

where, C_{ArC} is the concentration of aromatic compounds in the products.

3. Results and Discussion

3.1. Characterizations of Catalysts

Figure 2 presents the N_2 adsorption–desorption isotherms (Figure 2a) and the corresponding pore size distributions (Figure 2b) of the parent ZSM-5 and the metal-modified catalysts. The associated textural parameters are summarized in Table 1. As shown in Figure 2a, both ZSM-5 and the metal-modified catalysts exhibit a sharp N_2 uptake at low relative pressures ($p/p_0 < 0.1$), confirming that the intrinsic microporous framework of ZSM-5 is preserved after metal incorporation. No significant distortion in the isotherm shape is observed, indicating that the zeolite structure remains intact. Compared with the parent ZSM-5, the metal-loaded samples (ZnLaFe/ZSM-5 and ZnLaFeP/ZSM-5) show a noticeably lower N_2 uptake over the entire pressure range, suggesting a decrease in accessible pore volume and surface area. This behavior is consistent with partial pore blocking and surface coverage of the zeolite by deposited metal species.

The pore size distribution curves shown in Figure 2b further support these observations. All samples display a dominant pore size centered at approximately 3.4–3.6 nm, indicating that the overall pore size distribution remains essentially unchanged after metal loading. Nevertheless, the intensity of the pore volume peak decreases

Table 1. Textural characteristics of samples.

Catalysts	S_{BET}, m²/g	Pore volume, cm³/g	Pore diameter, nm
ZSM-5	340.0	0.35	3.6
ZnLaFe/ZSM-5	295.0	0.25	3.4
ZnLaFeP/ZSM-5	260.0	0.22	3.5

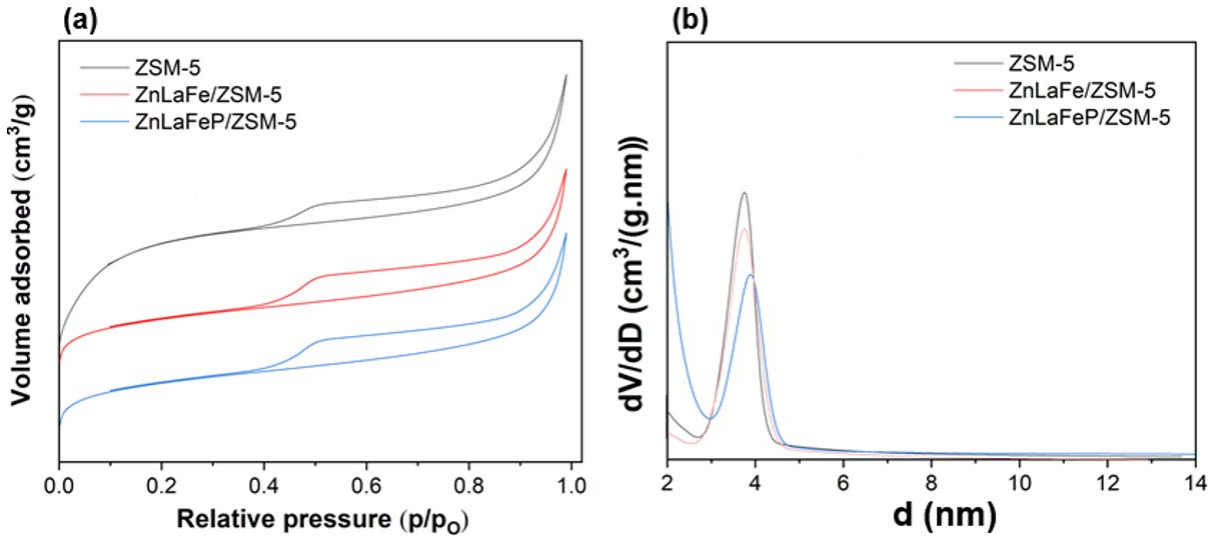

Figure 2. N_2 adsorption–desorption isotherms (a) and pore size distribution (b) of ZSM-5 and catalysts.

Copyright © 2026, ISSN 1978-2993

progressively from ZSM-5 to ZnLaFe/ZSM-5 and ZnLaFeP/ZSM-5, reflecting a reduction in pore volume rather than any structural collapse of the zeolite framework.

Figure 3 presents the XRD patterns of the parent ZSM-5 and the metal-modified catalysts. The diffraction peaks at 2θ = 7.96° and 8.83°, corresponding to the (011) and (200) planes, along with the reflections at 2θ = 23.18°, 23.32°, and 23.99°, assigned to the (501), (051), and (303) planes, are characteristic of calcined high-purity HZSM-5 with an MFI framework [32]. The unchanged peak positions and relative intensities following metal modification indicate that the crystallinity and structural integrity of the ZSM-5 framework are well preserved. Both ZnLaFe/ZSM-5 and ZnLaFeP/ZSM-5 retain the characteristic MFI-type diffraction features without the appearance of additional crystalline phases, indicating that the incorporation of Zn, La, Fe, and P does not disturb the zeolite framework.

Figure 4 displays the SEM micrographs and corresponding EDX spectra of (a) the parent ZSM-5, (b) ZnLaFe/ZSM-5, and (c) ZnLaFeP/ZSM-5 catalysts. The SEM images reveal that all samples preserve the characteristic morphology of ZSM-5, with well-defined crystal shapes and no evident structural degradation after metal and phosphorus modification. No significant particle agglomeration or framework collapse is observed, indicating that the preparation procedures do not adversely affect the zeolite structure. Moreover, the corresponding EDX spectra confirm the elemental composition of the catalysts. In addition to Si and Al originating from the ZSM-5 framework, the presence of Zn, La, and Fe in the modified samples verifies the successful incorporation of the metal species. For ZnLaFeP/ZSM-5, the additional detection of phosphorus further confirms effective P introduction. The relatively uniform elemental distribution and the absence of impurity signals suggest good dispersion of the deposited species on the zeolite support.

The SEM image of the untreated ZSM-5 (Figure 4a) shows irregularly shaped microcrystalline aggregates with relatively smooth surfaces, characteristic of commercial ZSM-5 morphology. No noticeable agglomeration or surface roughening is observed, indicating the pristine structure of the zeolite. The corresponding EDX spectrum mainly exhibits intense peaks of Si and O, with a small Al peak, consistent with the SiO_2-Al_2O_3 framework of ZSM-5. No additional metal peaks are detected, confirming the purity of the parent material. After the incorporation of Zn, La, and Fe (Figure 4b), the catalyst surface becomes rougher, and the particles appear more aggregated, suggesting that metal deposition slightly modifies the external surface of the zeolite crystals. The increased surface irregularity may be attributed to the dispersion of metal oxides on the zeolite surface. The EDX spectrum confirms the successful loading of Zn, La, and Fe onto ZSM-5, as evidenced by the appearance of characteristic peaks for these elements in addition to Si, O, and Al. The detected metal intensities demonstrate that the metals are well-dispersed within the analyzed region. The introduction of phosphorus further alters the morphology (Figure 4c), producing a more compact and densely aggregated surface compared to the metal-loaded sample without P. This suggests that phosphorus addition may promote stronger interactions between metal species and the support, leading

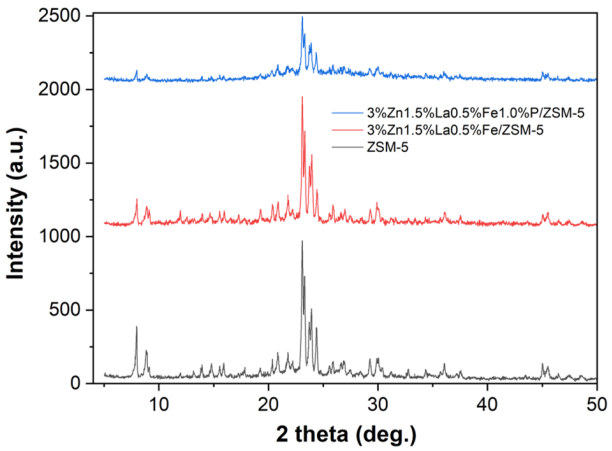

Figure 3. XRD pattern for SZM-5 and promoted catalysts.

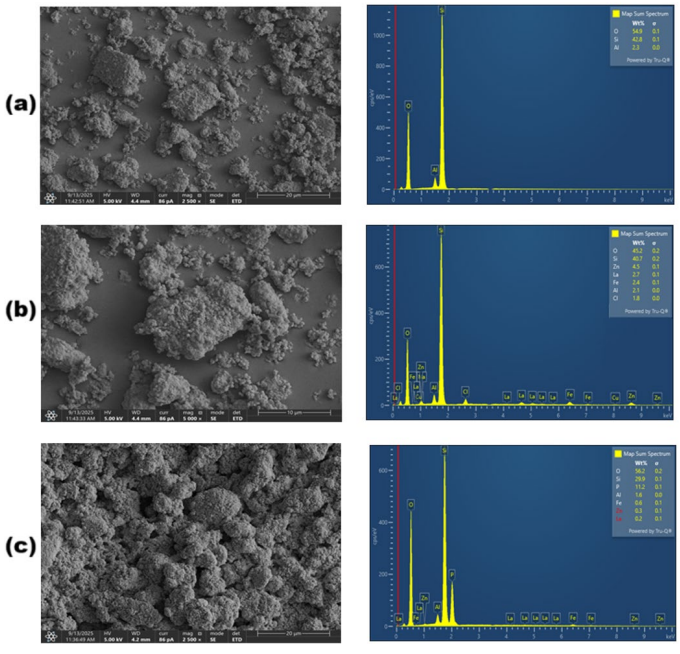

Figure 4. SEM images and the corresponding EDX spectra of catalysts: (a) ZSM-5, (b) ZnLaFe/ZSM-5 and ZnLaFeP/ZSM-5.

Copyright © 2026, ISSN 1978-2993

to enhanced surface coverage. The EDX spectrum clearly displays peaks corresponding to Zn, La, Fe, and P, confirming the incorporation of all added components. The presence of P is particularly notable, indicating successful modification and supporting the hypothesis that phosphorus influences metal dispersion and surface acidity. The micrographs of the ZnLaFe/ZSM-5 and ZnLaFeP/ZSM-5 catalysts, captured using the TEM, are presented in Figures 5a and 5b. The micrographs highlight the successful incorporation of the metal nanoparticles without significant agglomeration, indicating a well-controlled synthesis process for both catalysts.

Table 2 presents the acid properties of ZnLaFe/ZSM-5 and ZnLaFeP/ZSM-5 catalysts determined by NH_3-TPD analysis. Both catalysts exhibited weak, medium-strong, and strong acid sites; however, phosphorus incorporation significantly modified the acidity distribution and reduced the total acidity of the catalyst. The ZnLaFe/ZSM-5 catalyst showed a total acidity of 3520 µmol/g, mainly dominated by weak acid sites (2260 µmol/g), together with medium-strong (780 µmol/g) and strong acid sites (480 µmol/g). After phosphorus addition, the total acidity decreased to 2793 µmol/g in ZnLaFeP/ZSM-5. In particular, the amount of weak acid sites decreased from 2260 to 1700 µmol/g, while the concentration of strong acid sites decreased from 480 to 411 µmol/g. This reduction in strong acidity suggests that phosphorus species interact with framework aluminum and bridging hydroxyl groups, resulting in partial neutralization of strong Brønsted acid sites [33,34].

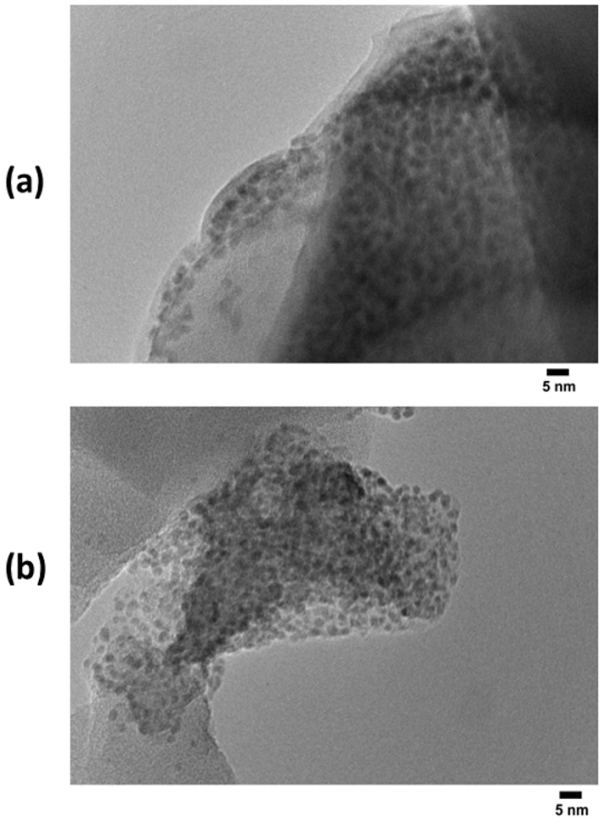

Figure 5. TEM images of the catalysts: (a) ZnLaFe/ZSM-5 and (b) ZnLaFeP/ZSM-5.

After incorporation of metal species (Zn, La, Fe), the total acidity decreases and the distribution shifts toward a higher proportion of medium-strength acid sites, which is attributed to metal–framework interactions and partial modification of Brønsted acid sites into Lewis-type centers. In particular, Zn species are reported to generate Lewis acid sites that are highly active for dehydrogenation and aromatization pathways, improving hydrocarbon conversion selectivity [35]. The reduction of strong acid sites is highly beneficial for aromatization reactions because excessive strong acidity in ZSM-5 promotes secondary cracking, hydrogen transfer reactions, and coke deposition, leading to rapid catalyst deactivation. Phosphorus modification improves catalyst stability by moderating the acidity and suppressing the formation of coke precursors [36].

3.2. Propane-Butane Conversion on Catalysts

The influence of reaction temperature on PBF conversion and product distribution over ZnLaFe/ZSM-5 and ZnLaFeP/ZSM-5 at a GHSV of 350 h^{-1} is presented in Table 3. The ZnLaFe/ZSM-5 catalyst shows high conversion across all temperatures and reaches its maximum aromatic yield at 550-600 °C. After phosphorus modification, the ZnLaFeP/ZSM-5 catalyst shows a noticeable decrease in conversion at lower temperatures, whereas at higher temperatures it provides a higher aromatic yield. It can be seen that both catalysts achieve their highest aromatic yields at 550 °C. The improved aromatic formation over the P-containing catalyst arises from the

Table 2. Acid properties of catalysts.

Sample	Weak acid		Medium-strong acid		Strong acid		ΣNH_3 (µmol/g)
	T, °C	Weak acid amount (µmol/g)	T, °C	Medium-strong acid amount (µmol/g)	T, °C	Strong acid amount (µmol/g)	
ZnLaFe/ZSM-5	115	2260	320	780	470	480	3520
ZnLaFeP/ZSM-5	135	1700	300	741	440	411	2793

Copyright © 2026, ISSN 1978-2993

modified acidity of the ZSM-5 framework, which shifts the product distribution away from cracking and towards the generation of larger aromatic compounds. The presence of P also stabilizes $Zn(OH)^+$ species within the modified acid environment, improving their effectiveness in aromatization [37,38].

The Py-FTIR spectra shown in Figure 6 indicate the presence of both Lewis and Brønsted acid sites on all catalysts. The band at approximately 1450 cm^{-1} is attributed to pyridine coordinated to Lewis acid sites, whereas the band near 1540 cm^{-1} corresponds to pyridinium ions formed on Brønsted acid sites [39]. The ZnLaFe/ZSM-5 catalyst exhibits a significant increase in the intensity of the Lewis acid band compared with the parent ZSM-5, suggesting the generation of additional Lewis acid centers associated with Zn species. Huyen *et al.* studies have demonstrated that Zn incorporation into ZSM-5 decreases the concentration of Brønsted acid sites while creating new Lewis acid sites that act as active centers for alkane dehydrogenation and aromatization [40]. The incorporation of phosphorus into ZnLaFeP/ZSM-5 catalyst further tailors the acidity distribution, resulting in an increased concentration of Lewis acid sites accompanied by a corresponding decrease in Brønsted acid sites (Figure 6). These results are in good agreement with the NH_3-TPD data presented in Table 2 and clearly demonstrate that phosphorus modification leads to a reduction in the total acidity of the catalyst, as well as a pronounced alteration in the distribution of acid strength. Phosphorus species interact with framework hydroxyl groups and partially neutralize strong Brønsted acid sites while stabilizing zinc-containing Lewis acid centers. Meanwhile, excessive Brønsted acidity favors secondary cracking, hydrogen-transfer reactions, and dealkylation of alkyl aromatics, leading predominantly to benzene and toluene formation. Therefore, the reduction of strong Brønsted acid sites by phosphorus suppresses these undesired reactions and preserves alkyl-substituted aromatics, particularly xylenes [41].

The catalytic results presented in Table 3 clearly demonstrate the influence of acid-site distribution on the aromatization of the propane–butane fraction. For ZnLaFe/ZSM-5, the aromatic yield reaches 35.6% at 550 °C, with benzene and toluene accounting for 40.7% and 47.0% of the aromatic products, respectively, while the xylene selectivity remains low at 3.3%. In contrast, ZnLaFeP/ZSM-5 achieves a higher aromatic yield of 59.1% under the same conditions, accompanied by a increase in xylene selectivity to 29.2%. This behavior can be attributed to the synergistic effect of enhanced Lewis acidity and moderated Brønsted acidity. Lewis acid sites associated with Zn species promote the dehydrogenation of propane and butane to olefinic intermediates, which subsequently undergo oligomerization, cyclization, and dehydrogenation to form aromatic compounds. Several studies have identified Zn-derived Lewis acid sites as the principal active centers responsible for alkane aromatization over ZSM-5-based catalysts [42].

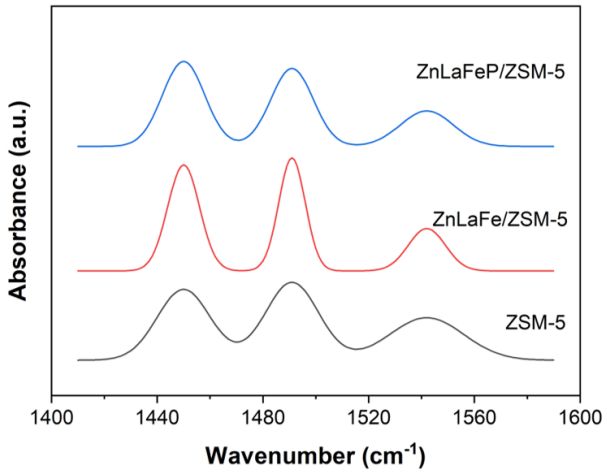

Figure 6. FTIR spectra of pyridine adsorbed of ZSM-5 and catalysts.

Table 3. Conversion of PBF over the obtained catalysts at GHSV = 350 h^{-1}. Note: X- conversion of PBF, %; Y- Yield of aromatic compounds, %.

T,°C	X, %	Y, %	Composition of products, %				
			Benzene	Toluene	Ethylbenzene	Xylene	C_{8+}
ZnLaFe/ZSM-5							
450	74.4	28.4	13.5	60.6	15.7	6.9	2.1
500	84.5	31.4	30.7	45.9	14.9	5.6	2.9
550	87.3	35.6	40.7	47.0	8.4	3.3	0.6
600	91.2	28.1	45.2	48.1	5.5	2.5	0
ZnLaFeP/ZSM-5							
450	27.2	55.8	6.2	40.1	23.9	17.9	11.9
500	58.2	56.2	14.5	47.4	13.9	17.5	6.7
550	88.3	59.1	20.4	36.8	7.4	29.2	6.2
600	87.4	56.8	17.6	39.7	4.5	18.9	19.3

Copyright © 2026, ISSN 1978-2993

Figure 7 illustrates the proposed reaction pathway for the aromatization of alkane fractions, such as propane and butane, over ZSM-5-based catalysts, leading to the formation of valuable aromatic hydrocarbons such as benzene and toluene [43]. Initially, alkanes are activated by C-H bond breakage, dehydrogenation, and C-C cracking reactions on the catalyst's acidic and metallic active sites, resulting in lower alkenes, hydrogen, and lighter alkane species. Higher alkene intermediates are produced when these lower olefins take part in oligomerization and cracking events that are mediated by Brønsted acid sites (H^+) inside the ZSM-5 framework. The higher alkenes proceed through cyclization, hydrogen transfer, and dehydrogenation processes in the last stage, which results in the production of aromatic compounds like benzene, toluene, xylene, and heavier C_4^+ aromatics. While the acidic zeolite framework encourages oligomerization and aromatization pathways, the presence of metal promoters in ZSM-5 increases dehydrogenation activity and makes hydrogen removal easier. Overall, it was demonstrated that the synergistic role of metal and acid sites in converting propane–butane feedstocks into high-value aromatic hydrocarbons through sequential cracking, oligomerization, and aromatization reactions.

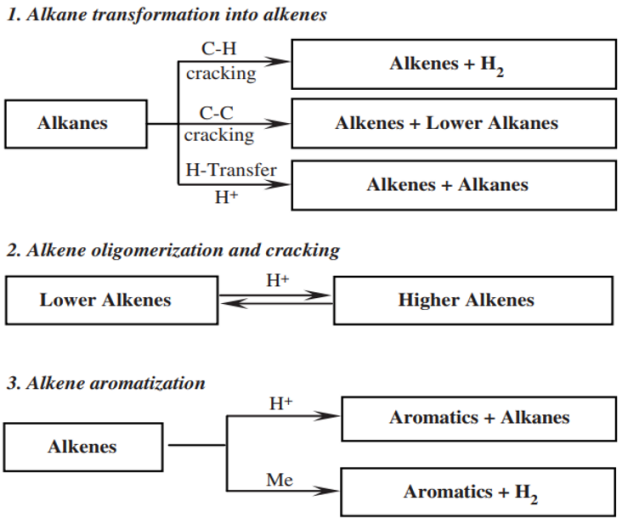

Figure 7. Schematic illustration of alkane aromatization over Me,H-ZSM-5 catalysts. Reproduced with permission from Ref. [43].

The substantially higher aromatic yield and xylene selectivity observed over ZnLaFeP/ZSM-5 suggest that an optimized Lewis-to-Brønsted acid site ratio is highly beneficial for propane–butane aromatization. Similar observations have been reported in the literature, where phosphorus modification of ZSM-5 improved xylene selectivity by reducing strong Brønsted acidity, while Zn-derived Lewis acid sites enhanced dehydrogenation and aromatization activity [44]. Long *et al.* demonstrated that the incorporation of phosphorus (P) into ZSM-5 promotes the formation and stabilization of zinc species within the support structure, leading to a significant improvement in catalyst stability. Moreover, the synergistic interaction between La and P was found to increase the concentration of active $[Zn(OH)]^+$ species, which in turn enhances aromatization activity and further improves the overall stability of the catalyst. Consequently, the superior performance of ZnLaP/ZSM-5 can be attributed to the combined effects of increased Lewis acidity, enhanced dehydrogenation capability, and suppression of excessive cracking and dealkylation reactions, resulting in higher yields of BTX aromatics and particularly xylene-rich products [45].

The PBF conversion over ZnLaFe/ZSM-5 and ZnLaFeP/ZSM-5 at 550 °C under different GHSV conditions is summarised in Table 4. For ZnLaFe/ZSM-5, increasing GHSV from 140 to 350 h^{-1} lowers the conversion from 88.3 to 71.8% while the aromatic fraction becomes more pronounced.

Table 4. Conversion of PBF over the obtained catalysts at T = 550 °C. Note: X- conversion of PBF, %; Y- Yield of aromatic compounds, %.

GHSV, h^{-1}	X, %	Y, %	Composition of products, %				
			Benzene	Toluene	Ethylbenzene	Xylene	C_{8+}
ZnLaFe/ZSM-5							
140	88.3	49.1	18.7	73.1	6.6	1.6	0
350	76.1	33.6	39.7	46.4	10.0	3.2	0.7
450	72.7	24.3	19.9	67.7	10.0	2.4	0
500	71.8	20.7	19.3	70.8	7.6	2.3	0
ZnLaFeP/ZSM-5							
140	80.2	54.7	26.4	45.0	3.8	3.1	8.2
350	88.3	59.1	21.2	40.2	4.1	10.9	9.2
450	80.0	47.1	21.4	46.8	4.0	4.4	6.6
500	69.6	33.1	22.3	48.3	3.9	3.4	5.8

Copyright © 2026, ISSN 1978-2993

The benzene yield reaches 39.7% and the total aromatic yield is 33.6%. For ZnLaFeP/ZSM-5, the highest total aromatic yield of 59.1% and the largest C_{8+} fraction of 9.2% occur at 350 h^{-1}, and both values decrease at higher GHSV. The enhanced performance of the P-modified catalyst is consistent with the reduction of strong Brønsted acid sites upon P incorporation, which suppresses excessive cracking and favours pathways leading to heavier aromatic products [46]. The obtained data indicate that 350 h^{-1} provides a contact time that allows the primary conversion steps and subsequent aromatization to proceed efficiently, resulting in more effective formation of aromatic products on both catalysts.

The ZnLaFeP/ZSM-5 catalyst outperforms standard Zn-, Ga-, Pt-, and Mo-modified ZSM-5 catalysts in the conversion of propane-butane fraction (PBF) to aromatic hydrocarbons. Specifically, at moderate GHSV, the phosphorus-modified catalyst produced the maximum aromatic yield, while encouraging the production of heavier C_4^+ aromatic compounds. Phosphorus likely suppresses excessive cracking reactions and improves selective aromatization routes by lowering the concentration of strong Brønsted acid sites. The ZnLaFeP/ZSM-5 catalyst is a potential catalyst for effective LPG aromatization and value-added aromatic hydrocarbon synthesis because it exhibits a better balance between conversion, aromatic selectivity, and heavier hydrocarbon production when compared to traditional Zn/ZSM-5 and La/ZSM-5 systems (Table 5).

According to the data in Table 6, the ZnLaFeP/ZSM-5 catalyst exhibits consistently higher conversion and aromatic yield throughout the 11 h stability test compared with ZnLaFe/ZSM-5. The conversion over ZnLaFeP/ZSM-5 remains in the range of 83.7–88.3%, whereas that of ZnLaFe/ZSM-5 varies between 78.9 and 83.5%. A similar trend is observed for the aromatic yield: ZnLaFeP/ZSM-5 achieves values of 49.7–59.7%, while ZnLaFe/ZSM-5 yields remain limited to 30.0–32.5%. Notably, even the lowest aromatic yield obtained over ZnLaFeP/ZSM-5 exceeds the highest value observed for ZnLaFe/ZSM-5. These results demonstrate that, under the applied reaction conditions, ZnLaFeP/ZSM-5 maintains superior catalytic performance and stability.

The stability of the ZnLaFeP/ZSM-5 catalyst during propane–butane fraction conversion was evaluated over 11 h of continuous operation (Table 6). Only minor decreases in propane–butane conversion, from 88.3% to 83.7%, and in aromatic yield, from 59.7% to 49.7%, were observed during the time-on-stream experiment, confirming the catalyst's high resistance to deactivation. Gou et al. studies have reported that phosphorus

Table 5. Benchmark comparison of PBF aromatization performance over ZSM-5-based catalysts.

Catalyst	Temperature (°C)	GHSV (h^{-1})	Conversion (%)	Aromatic Yield (%)	Main Aromatic Products	Advantages	Disadvantages	Ref.
ZnLaFe/ZSM-5	550	140	88.3	49.1	Toluene-rich aromatics	High PBF conversion and strong toluene selectivity	Lower C_8^+ aromatic formation and higher cracking tendency	This work
ZnLaFeP/ZSM-5	550	350	88.3	59.1	Toluene, xylene, and C_8^+ aromatics	Highest aromatic yield and improved heavier aromatic production due to P modification	Slightly lower benzene selectivity	This work
Zn/ZSM-5	500–550	300–600	60–85	35–50	Benzene, toluene, xylene (BTX)	Good aromatization activity and established catalyst system	Catalyst deactivation by coke deposition	[19]
Ga/ZSM-5	500–580	500–1500	70–95	45–65	BTX aromatics	Excellent dehydrogenation and aromatization performance	Gallium is relatively expensive	[47]
Pt/ZSM-5	450–550	1000–3000	75–98	50–70	BTX and light aromatics	High stability and hydrogen transfer activity	Noble metal cost and sensitivity to sulfur impurities	[48]
Mo/HZSM-5	600–700	500–1200	55–80	40–60	Benzene and toluene	Strong aromatization ability at high temperature	Rapid coke formation under severe conditions	[49]
La/ZSM-5	500–550	300–800	65–82	35–48	Toluene and xylene	Improved catalyst stability and coke resistance	Moderate aromatic yield compared with bimetallic systems	[27]

Copyright © 2026, ISSN 1978-2993

incorporation into ZSM-5 reduces the concentration of excessively strong Brønsted acid sites, improves hydrothermal stability, and suppresses pore blockage by modifying coke deposition patterns [50].

The deactivation behavior of ZnLaFe/ZSM-5 and ZnLaFeP/ZSM-5 catalysts after 11 h of PBF aromatization was evaluated by thermogravimetric analysis, and the results are presented in Figure 8. Both catalysts exhibited a continuous weight loss with increasing temperature, indicating the combustion of deposited carbonaceous species formed during the reaction. However, the amount of weight loss differed between the two samples. In both catalysts, an initial weight loss below approximately 200 °C can be attributed to the removal of physically adsorbed water associated with the zeolite pores. The subsequent weight loss observed between 400 and 700 °C is mainly associated with the combustion of coke species deposited on the catalyst surface and within the pore structure. TGA analysis revealed lower coke deposition on ZnLaFeP/ZSM-5 compared with ZnLaFe/ZSM-5. This improvement is attributed to phosphorus-induced mesoporosity, which enhances mass transfer, suppresses the accumulation of coke precursors, and consequently improves catalyst stability during aromatization.

For evaluation of scalability, larger batches of the ZnLaFeP/ZSM-5 catalyst (100 mL and 500 mL) were synthesized and tested in a pilot-scale reactor for the conversion of a propane–butane fraction containing 40% propane and 60% butane from the JSC "Pavlodar Oil Refinery" (Kazakhstan). The experiments were conducted at a gas hourly space velocity of 350 h^{-1} and reaction temperatures up to 550 °C (Table 7). In both catalyst beds, the phosphorus-modified catalyst achieved the highest aromatic yields, reaching 35.9% for the 100 mL bed and 29.6% for the 500 mL bed, confirming that the optimized balance of acidity is retained upon scale-up.

Increasing the reaction temperature from 450 to 550 °C resulted in a significant increase in propane–butane conversion, from 42.6% to 67.8% for the 100 mL catalyst bed and from 36.6% to 93.7% for the 500 mL bed. This temperature-

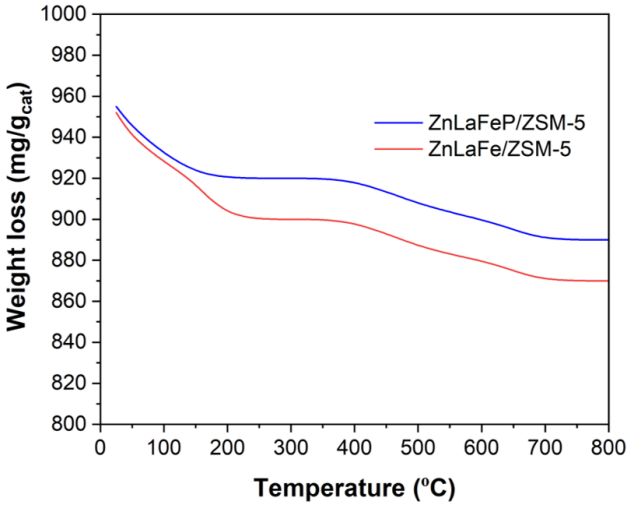

Figure 8. TGA profiles of the deactivated ZnLaFe/ZSM-5 and ZnLaFeP/ZSM-5 catalysts.

Table 6. Stability testing of the obtained catalysts in conversion of PBF at 550 °C, GHSV = 350 h^{-1}. Note: X- conversion of PBF, %; Y- Yield of aromatic compounds, %.

Catalyst running time, h	X, %	Y, %	Composition of products, %			
			Benzene	Toluene	Ethylbenzene	Xylene
ZnLaFe/ZSM-5						
1	81.1	30.9	36.6	43.8	15.5	4.1
2	78.9	32.5	33.0	45.5	14.2	7.3
3	79.0	31.5	31.6	45.9	14.5	8.0
5	80.2	30.0	32.7	47.0	12.5	7.8
7	81.2	32.0	32.2	46.0	13.8	8.0
9	83.1	32.2	31.8	45.8	13.9	7.9
11	83.5	31.5	31.5	45.1	13.1	7.5
ZnLaFeP/ZSM-5						
1	88.3	59.7	23.2	39.2	3.1	9.9
2	87.9	58.5	30.0	43.5	13.2	6.3
3	86.5	56.5	30.6	44.9	13.5	7.0
5	85.2	52.3	30.7	46.0	11.5	6.8
7	84.8	52.1	29.2	45.0	12.8	7.0
9	84.0	50.2	28.8	44.8	14.9	8.9
11	83.7	49.7	27.5	47.1	14.1	8.5

Copyright © 2026, ISSN 1978-2993

driven enhancement is attributed to the preserved synergy between moderated Brønsted acid sites and Zn–phosphate Lewis centers, which continue to promote dehydrogenation and cyclization pathways even in larger catalyst volumes. Although a slight decrease in aromatic selectivity was observed at higher catalyst loadings-likely due to increased diffusion limitations within the microporous structure-the catalyst maintained high overall activity, demonstrating the strong scalability and robustness of phosphorus-stabilized ZSM-5 catalysts for industrially relevant aromatization processes.

The stability of the 500 mL batch of ZnLaFeP/ZSM-5 catalyst was investigated during PBF conversion (Table 8). Over 10 h of continuous operation, the aromatic hydrocarbon yield decreased slightly from 20.7% to 13.1%, and the conversion dropped from 99.6% to 76.8%, while the qualitative composition of the liquid products remained essentially unchanged. This stability is attributed to the presence of phosphorus, which moderates strong Brønsted acid sites to suppress excessive cracking and coke formation, while the Zn–phosphate Lewis sites maintain active dehydrogenation and cyclization pathways. As a result, the catalyst sustains the sequential transformation of olefinic and cyclic intermediates into aromatics, preserving both activity and selectivity over prolonged operation [51].

4. Conclusion

Phosphorus-modified ZnLaFe/ZSM-5 catalysts demonstrate that precise control of zeolite acidity plays a crucial role in the efficient aromatization of propane–butane fractions. The addition of Zn, La, Fe, and phosphorus maintained the crystalline MFI structure of ZSM-5 while specifically modulating the concentration of medium-strong and strong Brønsted acid sites, according to structural characterisation. This alteration altered the catalytic reaction pathways by inhibiting excessive cracking reactions and boosting sequential dehydrogenation, oligomerization, cyclization, and aromatization activities, resulting in BTX and heavier aromatic compounds. ZnLaFe/ZSM-5 demonstrated a maximum propane–butane conversion of 88.3% with an aromatic yield of 49.1% at 140 h^{-1} in catalytic testing at 550 °C under various GHSV conditions, whereas the phosphorus-modified ZnLaFeP/ZSM-5 catalyst demonstrated a significantly enhanced aromatic yield of 59.1% at 350 h^{-1} along with the highest C_4^+ aromatic fraction of 9.2%. The phosphorus-free catalyst produced only 0.7% C_8^+ aromatics under comparable circumstances.

Additionally, the ZnLaFeP/ZSM-5 catalyst showed enhanced catalytic durability and resistance to deactivation by maintaining strong aromatic selectivity while restricting unwanted cracking routes. The stability of the acid site distribution and suppression of coke-forming reactions are responsible for the phosphorus-containing catalyst's improved performance.

Table 7. Conversion of PBF over the larger batches of the ZnLaFeP/ZSM-5 modified zeolite-containing catalyst (100 mL, 500 mL) catalyst at T=550 °C, GHSV = 350 h^{-1}.

ZnLaFe P/ZSM-5 V = 100 mL			ZnLaFe P/ZSM-5 V = 500 mL		
T, °C	X, %	Y, %	T, °C	X, %	Y, %
450	42.6	27.0	450	36.6	21.7
500	58.2	31.4	500	50.6	22.3
550	67.8	35.9	550	93.7	29.6

Table 8. Stability testing over the larger batches of the ZnLaFeP/ZSM-5 catalyst (500 mL) at T = 550 °C, GHSV = 350 h^{-1}.

Catalyst running time, h	X, %	Y, %	Composition of products, %			
			Benzene	Toluene	Ethylbenzene	Xylene
1	96.6	20.7	27.6	42.7	11.9	17.8
2	96.1	20.5	29.4	23.3	10.6	17.7
3	93.9	20.2	29.9	40.3	9.7	20.1
5	88.3	17.4	30.1	41.3	9.9	18.7
7	77.6	14.2	26.0	43.1	12.8	18.1
9	76.8	13.6	24.4	40.1	19.8	15.7
10	76.8	13.1	23.4	38.1	17.5	21.0

Copyright © 2026, ISSN 1978-2993

These results show that, under industrially relevant conditions, adjusting acidity through phosphorus incorporation and metal–zeolite interactions is an efficient method for enhancing the generation of aromatic hydrocarbons from light alkanes. Overall, this work demonstrates the tremendous potential of multimetallic ZSM-5 catalysts enhanced with phosphorus for effective and long-lasting propane-butane upgrading into aromatic hydrocarbons with added value.

Acknowledgment

The authors would like to thank PhD. Shaimardan Esbol (Satbayev University, Almaty, Kazakhstan) for his support in the characterization of the catalysts.

CRedit Author Statement

Author Contributions: Nurzhan Nurgaliyev: formal analysis. Nur-Sultan Mussa: writing – original draft. Seitkhan Azat: formal analysis. Rachid Amrousse: investigation. Kainaubek Toshtay: writing – original draft, methodology, investigation, data curation, conceptualization, writing – review & editing, supervision. All authors have read and agreed to the published version of the manuscript.

References

[1] Akhtar, M.N., Jermy, B.R., Ahmad, N. (2025). Catalytic performance of sustainable bifunctional GaZn/ZSM-5 catalyst for LPG Aromatization. *Molecular Catalysis*, 584, 115298. DOI: 10.1016/j.mcat.2025.115298.

[2] Dehertog, W.J.H., Fromen, G.F. (1999). A catalytic route for aromatics production from LPG. *Applied Catalysis A: General*, 189(1), 63–75. DOI: 10.1016/S0926-860X(99)00252-5.

[3] Ghosh, A.C., Patil, G.S., Dutta, N.N. (1994). Liquid membrane permeation of aromatic hydrocarbons in LPG condensate. *Fuel Processing Technology*, 38(1), 17–30. DOI: 10.1016/0378-3820(94)90040-X.

[4] Kaltschmitt, T., Deutschmann, O. (2012). Fuel Processing for Fuel Cells. *Advances in Chemical Engineering*, 41, 1–64. DOI: 10.1016/B978-0-12-386874-9.00001-4.

[5] Egazariyants, S. V., Karakhanova, N.K. (2009). Determination of aromatic hydrocarbons in petroleum jet fuels by capillary gas chromatography and high-performance liquid chromatography. *Moscow University Chemistry Bulletin,* 64(1), 32–37. DOI: 10.3103/S0027131409010076.

[6] Wang, H., Nguyen, T.D., Tsilomelekis, G. (2023). Propane oxidative dehydrogenation using CO2 over CrOx /Fe-CeO2 catalysts. *Catalysis Science & Technology*, 13(8), 2360-2369. DOI: 10.1039/D2CY01563C.

[7] Fridman, V.Z., Xing, R. (2017). Deactivation Studies of the $CrOx/Al_2O_3$ Dehydrogenation Catalysts under Cyclic Redox Conditions. *Industrial and Engineering Chemistry Research*, 56(28), 7937–7947. DOI: 10.1021/acs.iecr.7B01638.

[8] Jin, D., Xu, H., Zhu, J., Cheng, D. (2023). Activation of Cr_2O_3 for propane dehydrogenation by doping with Pt single-atom promotor. *Molecular Catalysis*, 551, 113624. DOI: 10.1016/j.mcat.2023.113624.

[9] Shan, Y., Hu, H., Fan, X., Zhao, Z. (2023). Recent progress in catalytic dehydrogenation of propane over Pt-based catalysts. *Physical Chemistry Chemical Physics*, 25(28), 18609–18622. DOI: 10.1039/D3CP01659E.

[10] Sun, M., Zhai, S., Weng, C., Wang, H., Yuan, Z.Y. (2024). Pt-based catalysts for direct propane dehydrogenation: Mechanisms revelation, advanced design, and challenges. *Molecular Catalysis*, 558, 114029. DOI: 10.1016/j.mcat.2024.114029.

[11] Pan, J., Bru, G., Carbó, J.J., Godard, C., Ricart, J.M. (2025). Propane Dehydrogenation Catalyzed by Pt Clusters (Pt2–Pt6) in Gas Phase and Supported on $g\text{-}C_3N_4$ and $\gamma\text{-}Al_2O_3$: A Theoretical Study. *ACS Omega*, 10(39), 46105–46114. DOI: 10.1021/acsomega.5C07626.

[12] Nerl, H.C., Plodinec, M., Götsch, T., Skorupska, K., Schlögl, R., Jones, T.E., Lunkenbein, T. (2024). In Situ Formation of Platinum-Carbon Catalysts in Propane Dehydrogenation. *Angewandte Chemie - International Edition*, 63(24), e202319887. DOI: 10.1002/anie.202319887.

[13] Zhou, H., Li, H., Wang, L., Chu, S., Liu, L., Liu, L., Qi, J., Ren, Z., Cai, A., Hui, Y., Qin, Y., Song, L., Qin, X., Shi, J., Hou, J., Ding, Y., Ma, J., Xu, S., Tao, X., Li, L., Yang, Q., Hu, B., Liu, X., Chen, L., Xiao, J., Xiao, F.S. (2025). Cobaltosilicate zeolite beyond platinum catalysts for propane dehydrogenation. *Nature Catalysis 2025 8:4*, 8(4), 357–367. DOI: 10.1038/s41929-025-01320-x.

[14] Sattler, J.J.H.B., Ruiz-Martinez, J., Santillan-Jimenez, E., Weckhuysen, B.M. (2014). Catalytic Dehydrogenation of Light Alkanes on Metals and Metal Oxides. *Chemical Reviews*, 114(20), 10613–10653. DOI: 10.1021/CR5002436.

[15] Liu, D., Cao, L., Zhang, G., Zhao, L., Gao, J., Xu, C. (2021). Catalytic conversion of light alkanes to aromatics by metal-containing HZSM-5 zeolite catalysts—A review. *Fuel Processing Technology*, 216, 106770. DOI: 10.1016/j.fuproc.2021.106770.

[16] Ono, Y. (1992). Transformation of Lower Alkanes into Aromatic Hydrocarbons over ZSM-5 Zeolites. *Catalysis Reviews*, 34(3), 179–226. DOI: 10.1080/01614949208020306.

Copyright © 2026, ISSN 1978-2993

[17] Wang, H., Shiju, N.R. (2025). A mini review on aromatization of n-alkanes. *Reaction Chemistry & Engineering*, 10(4), 768–776. DOI: 10.1039/D4RE00384E.

[18] Geng, R., Liu, Y., Gao, J., Guo, Y., Dong, M., Wang, S., Fan, W., Wang, J., Qin, Z. (2022). The migration of Zn species on Zn/ZSM-5 catalyst during the process of ethylene aromatization. *Catalysis Science & Technology*, 12(13), 4201–4210. DOI: 10.1039/D2CY00661H.

[19] Barzallo, D., Reinoso, M.A., Miranda, G., Romero, T., Franco, M., Palmay, P. (2024). Bifunctional Catalytic Performance of Zn/ZSM-5 in the Aromatization of LPG and the Conversion of Pyrolytic Gases from Recycled Polypropylene. *ChemEngineering,* 8(6), 108. DOI: 10.3390/chemengineering8060108.

[20] Pan, T., Ge, S., Yu, M., Ju, Y., Zhang, R., Wu, P., Zhou, K., Wu, Z. (2022). Synthesis and consequence of Zn modified ZSM-5 zeolite supported Ni catalyst for catalytic aromatization of olefin/paraffin. *Fuel*, 311, 122629. DOI: 10.1016/j.fuel.2021.122629.

[21] Ishihara, A., Kanamori, S., Hashimoto, T. (2021). Effects of Zn Addition into ZSM-5 Zeolite on Dehydrocyclization-Cracking of Soybean Oil Using Hierarchical Zeolite-Al_2O_3 Composite-Supported Pt/NiMo Sulfided Catalysts. *ACS Omega*, 6(8), 5509–5517. DOI: 10.1021/acsomega.0C05855.

[22] Dauda, I.B., Yusuf, M., Gbadamasi, S., Bello, M., Atta, A.Y., Aderemi, B.O., Jibril, B.Y. (2020). Highly Selective Hierarchical ZnO/ZSM-5 Catalysts for Propane Aromatization. *ACS Omega*, 5(6), 2725–2733. DOI: 10.1021/acsomega.9B03343.

[23] Oseke, G.G., Atta, A.Y., Mukhtar, B., El-Yakubu, B.J., Aderemi, B.O. (2022). Synergistic effect of Zn with Ni on ZSM-5 as propane aromatization catalyst: effect of temperature and feed flowrate. *Journal of Porous Materials,* 29(6), 1839–1852. DOI: 10.1007/S10934-022-01294-2.

[24] Kumar, N., Byggningsbacka, R., Lindfors, L.E. (1997). Aromatization ofn-butane over Ni-ZSM-5 and Cu-ZSM-5 zeolite catalysts prepared by using Ni and Cu impregnated silica, fiber. *Reaction Kinetics and Catalysis Letters*, 61(2), 297–305. DOI: 10.1007/BF02478386.

[25] Zhang, Y., Wang, J., Zhang, L., Wang, W., Li, J. (2024). Synthesis of Hollow Zn/ZSM-5 Nanosheets via Different Alkali Treatments with ZIF-8 as a Zn Source for Efficient Aromatization of Methanol. *Langmuir*, 40(52), 27455–27469. DOI: 10.1021/acs.langmuir.4C03739.

[26] Song, S., Li, T., Ju, Y., Li, Y., Lv, Z., Zheng, P., Duan, A., Wu, P., Wang, X. (2022). Lanthanum/Gallium-Modified Zn/ZSM-5 Zeolite for Efficient Isomerization/Aromatization of FCC Light Gasoline. *Industrial & Engineering Chemistry Research*, 61(27), 9667–9677. DOI: 10.1021/acs.iecr.2C01104.

[27] Oseke, G. G., Atta, A. Y., Mukhtar, B., Jibril, B. Y., Aderemi, B. O. (2020). Highly selective and stable Zn–Fe/ZSM-5 catalyst for aromatization of propane. *Applied Petrochemical Research*, 10(2), 55–65. DOI: 10.1007/S13203-020-00245-9.

[28] Abdelsayed, V., Shekhawat, D., Smith, M.W. (2015). Effect of Fe and Zn promoters on Mo/HZSM-5 catalyst for methane dehydroaromatization. *Fuel*, 139, 401–410. DOI: 10.1016/j.fuel.2014.08.064.

[29] Fan, H., Nie, X., Song, C., Guo, X. (2025). Identification of the synergistic promotion of P and CO_2 on propane dehydrogenation and aromatization over the Zn/P-ZSM-5 catalyst. *Catalysis Science & Technology*, 15(17), 5076–5089. DOI: 10.1039/D5CY00607D.

[30] Song, L., Navarro de Miguel, J.C., Komaty, S., Chung, S.H., Ruiz-Martínez, J. (2025). Role of Phosphorus on ZSM-5 Zeolite for the Methanol-to-Hydrocarbon Reaction. *ACS Catalysis*, 15(7), 5623–5639. DOI: 10.1021/acscatal.4C07064.

[31] Hajimirzaee, S., Soleimani Mehr, A., Kianfar, E. (2022). Modified ZSM-5 Zeolite for Conversion of LPG to Aromatics. *Polycyclic Aromatic Compounds*, 42(5), 2334–2347. DOI: 10.1080/10406638.2020.1833048.

[32] Treacy, M.M.J., Higgins, J.B. (2007). Collection of Simulated XRD Powder Patterns for Zeolites, Fifth Edition. *Collection of Simulated XRD Powder Patterns for Zeolites, Fifth Edition*, 1–485. DOI: 10.1016/B978-0-444-53067-7.X5470-7.

[33] Blasco, T., Corma, A., Martínez-Triguero, J. (2006). Hydrothermal stabilization of ZSM-5 catalytic-cracking additives by phosphorus addition. *Journal of Catalysis*, 237(2), 267–277. DOI: 10.1016/j.jcat.2005.11.011.

[34] Abubakar, S.M., Marcus, D.M., Lee, J.C., Ehresmann, J.O., Chen, C.Y., Kletnieks, P.W., Guenther, D.R., Hayman, M.J., Pavlova, M., Nicholas, J.B., Haw, J.F. (2006). Structural and Mechanistic Investigation of a Phosphate-Modified HZSM-5 Catalyst for Methanol Conversion. *Langmuir*, 22(10), 4846–4852. DOI: 10.1021/LA0534367.

[35] Rodríguez-González, L., Hermes, F., Bertmer, M., Rodríguez-Castellón, E., Jiménez-López, A., Simon, U. (2007). The acid properties of H-ZSM-5 as studied by NH_3-TPD and 27Al-MAS-NMR spectroscopy. *Applied Catalysis A: General*, 328(2), 174–182. DOI: 10.1016/j.apcata.2007.06.003.

[36] Li, J., Ma, H., Sun, Q., Ying, W., Fang, D. (2015). Effect of iron and phosphorus on HZSM-5 in catalytic cracking of 1-butene. *Fuel Processing Technology*, 134, 32–38. DOI: 10.1016/j.fuproc.2014.11.026.

[37] Jiang, S., Chang, C.W., Swann, W.A., Li, C.W., Miller, J.T. (2024). Pt_3Mn/SiO_2 + ZSM-5 Bifunctional Catalyst for Ethane Dehydroaromatization. *Catalysts*, 14(6), 365. DOI: 10.3390/catal14060365/S1.

Copyright © 2026, ISSN 1978-2993

[38] Wang, X., Li, C., Yang, J., Liu, Y., Hei, J., Huang, S., Gao, D. (2024). Production of aromatic hydrocarbons from catalytic fast pyrolysis of microalgae over Fe-modified HZSM-5 catalysts. *RSC Advances*, 14(50), 36970–36979. DOI: 10.1039/D4RA06815G.

[39] Zhao, G., Teng, J., Xie, Z., Jin, W., Yang, W., Chen, Q., Tang, Y. (2007). Effect of phosphorus on HZSM-5 catalyst for C_4-olefin cracking reactions to produce propylene. *Journal of Catalysis*, 248(1), 29–37. DOI: 10.1016/j.jcat.2007.02.027.

[40] Huyen, P.T., Trinh, V.D., Teresa Portilla, M., Martínez, C. (2021). Influence of boron promotion on the physico-chemical properties and catalytic behavior of Zn/ZSM-5 in the aromatization of n-hexane. *Catalysis Today*, 366, 97–102. DOI: 10.1016/j.cattod.2020.03.030.

[41] Védrine, J.C., Auroux, A., Dejaifve, P., Ducarme, V., Hoser, H., Zhou, S. (1982). Catalytic and physical properties of phosphorus-modified ZSM-5 zeolite. *Journal of Catalysis*, 73(1), 147–160. DOI: 10.1016/0021-9517(82)90089-6.

[42] Liu, J., He, N., Zhou, W., Lin, L., Liu, G., Liu, C., Wang, J., Xin, Q., Xiong, G., Guo, H. (2018). Isobutane aromatization over a complete Lewis acid Zn/HZSM-5 zeolite catalyst: performance and mechanism. *Catalysis Science & Technology*, 8(16), 4018–4029. DOI: 10.1039/C8CY00917A.

[43] Nguyen, L.H., Vazhnova, T., Kolaczkowski, S.T., Lukyanov, D.B. (2006). Combined experimental and kinetic modelling studies of the pathways of propane and n-butane aromatization over H-ZSM-5 catalyst. *Chemical Engineering Science*, 61(17), 5881–5894. DOI: 10.1016/J.CES.2006.05.017.

[44] Bai, Y., Niu, X., Du, Y.E., Chen, Y. (2023). Conversion of Methanol to Para-Xylene over ZSM-5 Zeolites Modified by Zinc and Phosphorus. *Molecules,* 28(13) DOI: 10.3390/molecules28134890.

[45] Long, H., Jin, F., Xiong, G., Wang, X. (2014). Effect of lanthanum and phosphorus on the aromatization activity of Zn/ZSM-5 in FCC gasoline upgrading. *Microporous and Mesoporous Materials*, 198, 29–34. DOI: 10.1016/j.micromeso.2014.07.016.

[46] Teimouri Sendesi, S.M., Towfighi, J., Keyvanloo, K. (2012). The effect of Fe, P and Si/Al molar ratio on stability of HZSM-5 catalyst in naphtha thermal-catalytic cracking to light olefins. *Catalysis Communications*, 27, 114–118. DOI: 10.1016/j.catcom.2012.06.013.

[47] Liu, R.L., Zhu, H.Q., Wu, Z.W., Qin, Z.F., Fan, W. Bin, Wang, J.G. (2015). Aromatization of propane over Ga-modified ZSM-5 catalysts. *Journal of Fuel Chemistry and Technology*, 43(8), 961–969. DOI: 10.1016/S1872-5813(15)30027-X.

[48] Shou, H., Dasari, P.R., Broekhuis, R.R., Mondal, A., Patel, A., Nguyen, C., Fickel, D.W. (2022). Cracking of Butane on a Pt/H-ZSM-5 Catalyst in the Presence of Hydrogen. *Industrial & Engineering Chemistry Research*, 61(14), 4763–4773. DOI: 10.1021/acs.iecr.1C04545.

[49] Uslamin, E.A., Saito, H., Sekine, Y., Hensen, E.J.M., Kosinov, N. (2021). Different mechanisms of ethane aromatization over Mo/ZSM-5 and Ga/ZSM-5 catalysts. *Catalysis Today*, 369, 184–192. DOI: 10.1016/j.cattod.2020.04.021.

[50] Gou, M.L., Wang, R., Qiao, Q., Yang, X. (2014). Effect of phosphorus on acidity and performance of HZSM-5 for the isomerization of styrene oxide to phenylacetaldehyde. *Applied Catalysis A: General*, 482, 1–7. DOI: 10.1016/j.apcata.2014.05.023.

[51] Gao, X., Tang, Z., Zhang, H., Liu, C., Zhang, Z., Lu, G., Ji, D. (2010). High performance phosphorus-modified ZSM-5 zeolite for butene catalytic cracking. *Korean Journal of Chemical Engineering*, 27(3), 812–815. DOI: 10.1007/S11814-010-0134-6..

Copyright © 2026, ISSN 1978-2993